ISSN 1615-9306 · JSSCCJ 43 (5) 847–1018 (2020) · Vol. 43 · No. 5 · March 2020 · D 10609

JSS

JOURNAL OF

SEPARATION SCIENCE

5|20

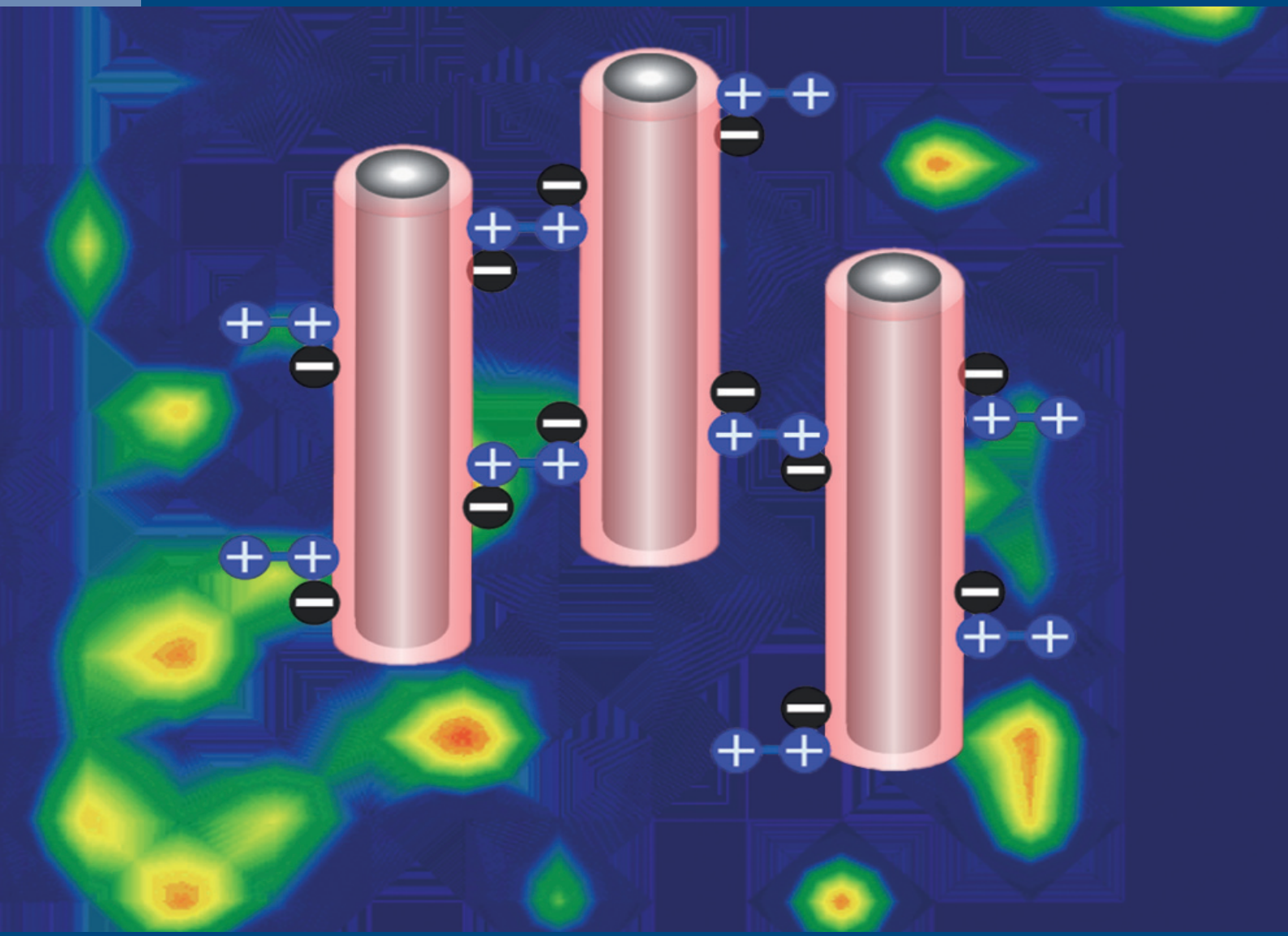

Methods
Chromatography · Electroseparation

Applications
Biomedicine · Foods · Environment

www.jss-journal.com

WILEY-VCH

Received: 5 October 2019 | Revised: 5 December 2019 | Accepted: 9 December 2019

DOI: 10.1002/jssc.201901024

RESEARCH ARTICLE

JOURNAL OF SEPARATION SCIENCE

Thermo-sensitive surface molecularly imprinted magnetic microspheres based on bio-macromolecules and their specific recognition of bovine serum albumin

Yufei Wang[1] | **Yong Ma**[2] | **Jingjing Zhou**[1] | **Kehe Su**[1] | **Baoliang Zhang**[1] | **Qiuyu Zhang**[1]

[1]MOE Key Laboratory of Material Physics and Chemistry under Extraordinary Conditions, School of Natural and Applied Science, Northwestern Polytechnical University, Xi'an, P. R. China

[2]School of Material Science and Engineering, Shandong University of Science and Technology, Qingdao, P. R. China

Correspondence
Professor Qiuyu Zhang, Northwestern Polytechnical University, Youyi Road 127#, Xi'an 710072, P. R. China.
Email: qyzhang@nwpu.edu.cn
Additional corresponding author: Dr. Baoliang Zhang
Email: blzhang@nwpu.edu.cn

Bovine serum albumin imprinted magnetic microspheres, with functional monomers of modified chitosan, *N*-isopropylacrylamide and sulfobetaine methacrylate, were successfully prepared and characterized in detail. Computational analyses showed that during the preparation process, modified chitosan can effortlessly form multiple non-covalent bonds with protein molecules. Temperature-sensitive *N*-isopropylacrylamide improves the elution efficiency by abating the mass transfer resistance. Meanwhile, the zwitterionic sulfobetaine methacrylate strongly interacts with H_2O molecules, remarkably reducing the non-specific adsorption. The specific bovine serum albumin adsorption performances of the prepared imprinted material were then determined. The adsorption amount reached 86.87 mg/g and the imprinting factor was 6.49. These excellent specific adsorption properties are attributed to the synergetic effects of the different monomers. The fabricated imprinted material not only exhibits great prospects as a biosensor or separation material for protein molecules, but also provides a collaborative strategy for preparing multi-functional imprinted materials.

KEYWORDS
chitosan, high adsorption, protein imprinted microspheres, responsiveness, selective recognition

1 | INTRODUCTION

Protein molecularly imprinted polymers (MIPs) are functionally polymeric materials that specifically recognize template proteins [1,2]. Thus far, MIPs have shown wide application prospects in many fields, such as chemical bionic sensors [3, 4], protein separation [5–7], natural antibody simulation [8–10], and drug sustained release [11,12]. However, the protein bio-macromolecules of the corresponding MIPs are disadvantaged by weak specificity of the functional groups, large size, and flexible conformations, which challenge their design and preparation [13,14]. For example, high-molecular-weight protein molecules cannot easily access the imprinted sites of the deep-coated MIPs [15]. The poor characteristics of functional groups and variable conformation of the protein molecules often degrade the MIP performance; specifically, they are responsible for the low adsorption amount and the low specific adsorption capacity of the MIP to its target protein [16].

To solve these problems, researchers have developed pioneering technologies and approaches such as surface imprinting technology, which does not require protein molecules to enter the deep layers of imprinted polymers. The shortcoming of this approach is the small effective separation site of the imprinted material, which reduces the separation efficiency below that of conventional bulk MIPs [17,18]. The transfer efficiency of protein molecules can be increased

Article Related Abbreviations: *IF*, Imprinting factor; LCST, lower critical solution temperature; MCS, modified chitosan; MIPs, Protein molecularly imprinted polymers; NIPAM, *N*-isopropylacrylamide; NIPs, Non-imprinted polymer microspheres; *Q*, Adsorption amount (mg/g); SBMA, sulfobetaine methacrylate; β, selection factor.

 © 2019 WILEY-VCH Verlag GmbH & Co. KGaA, Weinheim

by employing stimuli-responsive imprinted polymers as MIPs [19–21]. For example, temperature-sensitive MIPs can be rendered hydrophilic by a temperature change, favoring the elution of the protein molecules from the MIPs. In our previous research, we fabricated temperature-sensitive MIPs by decorating the surfaces of magnetic microspheres with *N*-isopropylacrylamide (NIPAM) and methyl methacrylate as the functional monomers. This construct effectively solved the difficulty of inserting/extracting the protein molecules into/from the MIPs [13], but the NIPAM functional monomer does not improve the adsorption amount and the imprinting factor of MIPs. Therefore, finding suitable functional monomers that enhance the performances of MIPs is urgently demanded.

Natural monomeric biomolecules such as dopamine and chitosan can obviously improve the performances of MIPs [22–24]. Modified chitosan (MCS) plays dual roles as a functional monomer and a cross-linking agent. The rich hydroxyl, amino, and carboxyl groups of MCS can effectively interact with protein molecules to increase the adsorption capacity of MIPs. Nevertheless, experiments have shown that although the MCS functional monomer indeed increases the adsorption capacity of MIPs, it does not improve the specific adsorption capacity. Sulfobetaine methacrylate (SBMA) can increase the specific adsorption [25,26], and NIPAM can endow the imprinted material with temperature sensitivity. Therefore, a protein imprinted material with both responsiveness and specificity has been prepared from an environmentally responsive macromolecular chain structure and an anti-protein adsorption structure, which attaches to the surface of the imprinted polymer.

2 | MATERIALS AND METHODS

2.1 | Materials

All chemicals were of analytical grade. BSA (MW 66.4 kDa, pI 4.7) and ovalbumin (OVA, MW 43.0 kDa, pI 4.7) were purchased from Amresco (Solon, OH, USA). Lysozyme (Lyz, MW 14.4 kDa, pI 11.0), bovine hemoglobin (BHb, MW 67 kDa, pI 6.8) and ribonuclease A (RNase A, MW 13.7 kDa, pI 7.8) were supplied by Sigma (St. Louis, MO, USA) and stored in a refrigerator before use. Chitosan was obtained from Alfa Aesar-Thermo Fisher Scientific (Tewksbury, MA, USA). *N*-isopropylacrylamide (NIPAM) was bought from Acros Organics (Morris Plains, NJ USA). SBMA was provided by J&K Chemicals (Shanghai, China). Glacial acetic acid, maleic anhydride, ammonium persulfate (APS), tetraethyl orthosilicate (TEOS), γ-methacryloxypropyltrimethoxysilane (KH-570, MPTS), Coomassie Brilliant Blue G-250 (Coomassie G), $NaHSO_3$, NaCl, $CaCl_2$, and $MgCl_2$ were obtained from commercial sources and used as received.

2.2 | Preparation of imprinted and non-imprinted polymer microspheres

To improve the water solubility of the product, chitosan with abundant hydroxyl and amino groups was modified with maleic anhydride to obtain MCS (Supporting Information S2) [27,28]. The recipe and characterization of MCS is described in the Supporting Information. The degree of substitution of MCS was 44.9%, and the introduced carboxyl content was 2.9646 mmoL/g. SiO_2/MPTS@Fe_3O_4 microspheres (0.1 g; see Supporting Information S1) were dispersed in a solution containing 0.03 g MCS, 0.02 g BSA, 0.05 g NIPAM, and 0.01 g SBMA. After shaking at 35°C for 30 min, the polymerization was started by adding 0.01 g APS and 0.01 g $NaHSO_3$ as the initiator. This mixture was stirried at 120 rpm for 24 h, yielding BSA-molecularly imprinted polymer microspheres (BSA-MIPs@SiO_2@Fe_3O_4, MIPs). The spheres were washed with 0.01% $CaCl_2$ to remove BSA from the imprinted sites. Non-imprinted polymer microspheres (NIPs@SiO_2@Fe_3O_4, NIPs) were prepared by the same method, but without adding BSA in the preparation. The prepared NIPs were also washed with 0.01% $CaCl_2$ for the same number of times. After lyophilization, the products were characterized and rebounded. Two 8 mg products as adsorbents were separately incubated in 5 mL protein solution (0.6 mg/mL, pH 7.0) at 35°C for 3.0 h.

2.3 | Imprinting parameter determination experiments

The imprinting parameters, namely, the adsorption amount (Q, mg/g), the imprinting factor (IF), and the selection factor (β) of the MIPs, were respectively calculated by the following three formulas:

$$Q = (C_0 - C_1)V/W, \tag{1}$$

$$IF = Q_{\mathrm{MIPs}}/Q_{\mathrm{NIPs}}, \tag{2}$$

$$\beta = IF_{\mathrm{T}}/IF_{\mathrm{C}}, \tag{3}$$

where C_0 (mg/mL) and C_1 (mg/mL) are the protein concentrations in the initial solution and after adsorption to the MIPs, respectively, detected at 595 nm on a UV–Vis spectrophotometer by Coomassie G staining [29,30]. V (mL) donates the volume of the adsorbed protein solution and W (g) is the dry weight of the adsorbent materials. IF and β reflect the specific recognition properties of MIPs. IF_{T}, and IF_{C} are the IFs of the template and competitive proteins, respectively.

2.4 | Characterization

The morphologies of the materials were observed by transmission electron microscope (TEM) imaging (JEM-3010 TEM, JEOL, Tokyo, Japan). Fourier transform infrared

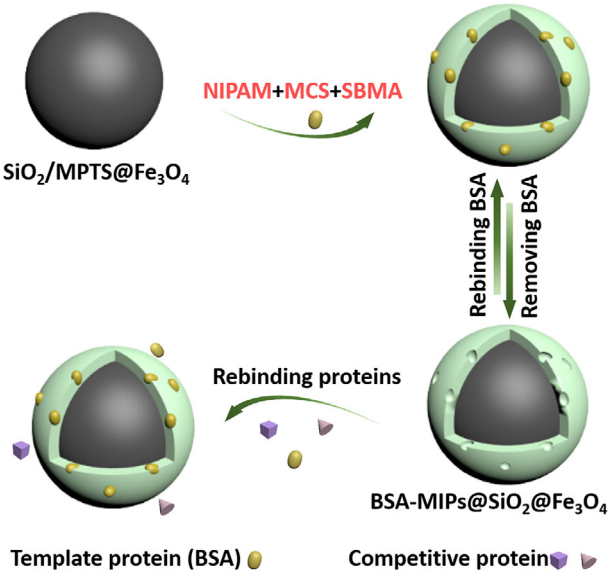

FIGURE 1 Schematic of BSA-MIPs@SiO_2@Fe_3O_4 synthesis, showing the adsorption mechanism at each step

(FTIR) spectra were recorded on a Tensor27 FTIR spectrometer (Bruker Optics, Ettlingen, Germany). The inorganic contents of the products were measured by thermogravimetric analysis (TGA) using a TGA2 thermogravimetric analyzer (Mettler Toledo, Columbus, OH, USA). The magnetic properties were evaluated from vibrating sample magnetometer (VSM) curves obtained on a LakeShore 7307 vibrating sample magnetometer (Lake Shore Cryotronics, Westerville, OH, USA). Finally, the protein contents were measured in a UV-2550 spectrophotometer at 35°C (Shimadzu, Kyoto, Japan).

3 | RESULTS AND DISCUSSION

3.1 | Fabrication of BSA specific adsorption material

Figure 1 shows the preparation process of the surface BSA MIPs. First, the SiO_2@Fe_3O_4 microspheres were fabricated by Stöber hydrolysis, followed by surface modification with many C=C bonds. Next, a BSA imprinted layer was formed on the modified microsphere surfaces by polymerizing the functional monomers NIPAM and MCS. Before the preparation process, the affinity of the monomers to the protein was demonstrated by a computational method. The crystal structure of BSA (PDBID: 4jk4) was taken as the initial 3D structure of the macromolecule for molecular docking. Using NIPAM and the unit structures of CS and MCS as ligands, the molecular docking was performed by the Ladmark genetic algorithm implemented in the Autodock 4.2 software package (Supporting Information S3). The binding free energies of the ligands to BSA are shown in Supporting Information Table S1. CS demonstrated the lowest binding free energy, followed by MCS and NIPAM. Because CS is insoluble in aqueous solution, MCS was chosen as the ligand.

The numerous hydroxyl groups on the MCS not only increase the water dispersibility of the MIPs, but also spontaneously form hydrogen bonds with the protein molecules. Therefore, the imprinted shell exhibited excellent absorption ability. Furthermore, the multiple double bonds attached to MCS, which also originate from the surface modification, acted as cross-linking agents through which the MCS macromolecular chains and NIPAM small molecules formed a networked cross-linking structure [31]. Once the polymerized NIPAM (PNIPAM) segment was formed, the adsorption and desorption performances of the obtained MIPs could be readily adjusted by changing the environmental temperature.

The size, shape and distribution of the imprinted cavities of the MIPs are complementary to those of the functional groups of BSA alone at an appropriate temperature (35°C). At temperatures below the lower critical solution temperature (LCST), PNIPAM is hydrophilic and the expanded imprinted cavities no longer complement the shape structure of the functional groups; accordingly, the specific adsorption on the protein molecules disappears. At temperatures above the LCST, PNIPAM is hydrophobic and the imprinting cavities shrink. In this case, protein molecules can be trapped by the hydrophobic interaction between the imprinted polymers and the shrunken imprinted cavities, impeding the protein transfer. Therefore, protein adsorption is favored at 35°C and protein elution is favored at temperatures below the LCST.

To study the effects of monomer content and cross-linking degree on the specific adsorption properties of the imprinted materials, MIPs and NIPs with different monomer contents were prepared (see Table 1). Increasing the amount of temperature-sensitive monomer NIPAM increased the Q, and initially increased the IF. At higher NIPAM concentrations, the IF decreased under the increased temperature response of the polymer. In this situation, the Q increased because the NIPAM facilitated the transfer of the protein molecules. On the other hand, increasing the amount of NIPAM decreased the crossing degree, which reduced the rigidity of the molecular chains. The increased flexibility of MCS molecules increased the ease of protein capture by both MIPs and NIPs. Meanwhile, for an imprinted material exposed to increasing temperature, the proportion of Q_{MIPs} increased less than that of Q_{NIPs}, so the IF increased and then decreased. As this rule was violated by the Q_{MIPs} and Q_{NIPs} of sample-1, it was speculated to be mainly caused by MCS. To check this speculation, sample-5 with no NIPAM was prepared as a control experiment. Both the Q_{MIPs} and Q_{NIPs} of this sample were elevated significantly with temperature. As NIPAM was absent in this sample, the MCS molecules were not completely cross-linked. MCS molecules floating freely on the microsphere surfaces can overstretch through the water,

TABLE 1 Adsorption amounts *Q* and imprinting factors *IF* of microspheres with different monomer contents (MCS, 30 mg)

Microspheres	NIPAM (mg)	SBMA (mg)	Q_{MIPs} (mg/g)	Q_{NIPs} (mg/g)	*IF*
Sample-1	20	0	135.74	66.21	2.05
Sample-2	30	0	108.15	43.11	2.51
Sample-3	40	0	128.16	45.34	2.83
Sample-4	50	0	138.25	52.82	2.62
Sample-5	0	0	223.2	204.4	1.09
Sample-6	30	10	70.31	20.25	3.47
Sample-7	40	10	103.21	23.49	4.39
Sample-8	50	10	114.97	30.89	3.72
Sample-9	40	20	86.87	13.38	6.49

thereby capturing many more protein molecules than cross-linked MCS molecules. However, the obviously declining *IF* indicates an inferior specific adsorption capacity. To reduce the non-specific adsorption of imprinted microspheres, we added 10 mg SBMA to samples prepared under the same reaction conditions as Sample-2, Sample-3, and Sample-4, thereby obtaining Sample-6, Sample-7, and Sample-8, respectively. The *IF* obviously increased from 2.51, 2.03, and 2.62 in Samples 2, 3, and 4, respectively to 3.47, 4.39, and 3.72 in Samples 6, 7, and 8, respectively. The *IF* improved because the non-specific adsorption decreased much faster than the specific adsorption. With no imprinting sites, NIPs lack a specific adsorption capability. In MIPs, the SBMA blocks the non-specific adsorption without destroying the imprinted cavities that adsorb specific proteins. Consequently, the anti-protein effect of SBMA is instrumental in reducing the non-specific adsorption capacity. Increasing the amount of SBMA to 20% (thereby obtaining Sample-9) further reduced the non-specific adsorption. The *IF* of Sample-9 was raised to 6.46.

To test the elution performance of the temperature-sensitive imprinted polymer, 0.1 M NaCl, $CaCl_2$ and $MgCl_2$ buffer solutions were selected as the eluents of BSA at 25°C. As shown in Figure 2, $CaCl_2$ solution delivered the highest elution efficiency (84.1%), so $CaCl_2$ solutions of varying concentrations were prepared for further elution studies. As the $CaCl_2$ concentration increased from 0.01 to 0.5 M, the elution efficiency first increased and then decreased. Ca^{2+} destroys the interaction between protein molecules and MIPs, thereby releasing the protein molecules into the elution. However, it also interacts with the carboxyl group of MCS to form a physical cross-linked structure. Thus, high concentrations of Ca^{2+} actually impede the elution of protein molecules. To weaken the effect of the physical cross-linked structure, some elution efficiency must be sacrificed, so 0.01 M $CaCl_2$ solution was chosen as the eluent. To illuminate the effect of temperature on elution efficiency, the elution performances in 0.01 M $CaCl_2$ solution were compared at 35 and 25°C. The elution efficiency declined from 75.1% at 25°C to 53.6% at 35°C. This result convincingly demonstrates that the temperature response improves the adsorption and elution abilities of the imprinted polymer.

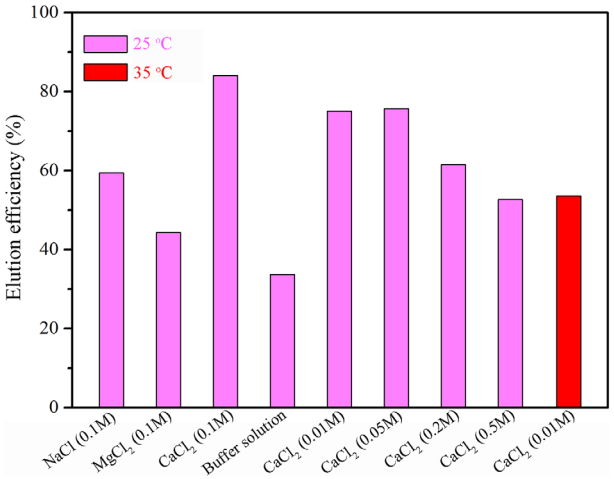

FIGURE 2 Elution efficiencies of different eluents in one instance

3.2 | Characterization

Figure 3 shows the TEM images of SiO_2@Fe_3O_4, Sample-9-MIPs and Sample-9-NIPs. The hierarchical structure of these samples was obscured by the similar contrasts of the SiO_2 and polymer. At high magnification (Figure 3A, inset), SiO_2@Fe_3O_4 exhibited a two-layered structure with an outer coating of approximately 30 nm. However, as shown in the insets of Figure 3B and C respectively, the MIPs and NIPs clearly presented a three-layered structure with an outer shell thickness of approximately 11 nm. These visual images verify the successful coating of the polymer shell on the surfaces of the SiO_2@Fe_3O_4 microspheres.

From the FTIR spectra (Supporting Information Figure S7), new functional groups represent -CON stretching (1649 cm^{-1}) and -N–H formation (1539 cm^{-1}) of Sample-9-MIPs, confirming that the polymer layer had formed on the SiO_2@Fe_3O_4 microspheres. Supporting Information Figure S8 presents the TGA curves of SiO_2/MPTS@Fe_3O_4,

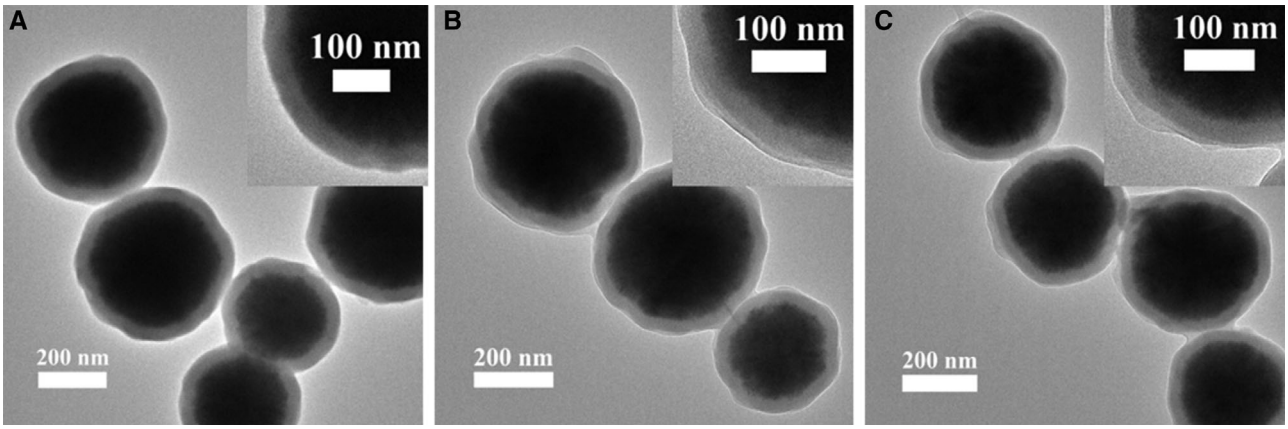

FIGURE 3 TEM images of (A) SiO_2@Fe_3O_4, (B) Sample-9-MIPs and (C) Sample-9-NIPs

Sample-9-MIPs and Sample-9-NIPs. The ultimate inorganic contents of SiO_2/MPTS@Fe_3O_4, Sample-9-MIPs and Sample-9-NIPs were 94.9, 80.8 and 82.9%, respectively. The specific saturation magnetization is an important performance index of magnetic composite microspheres. A higher specific saturation magnetization indicates a higher susceptibility to magnetic separation in the material. The specific saturation magnetizations of SiO_2@Fe_3O_4, Sample-9-MIPs and Sample-9-NIPs were 59.2, 38.3, and 45.8 emu/g, respectively (Supporting Information Figure S9).

3.3 | Saturated adsorption properties and kinetics study

To investigate the adsorption capability of Sample-9-MIPs and Sample-9-NIPs for BSA, the saturated adsorption properties were measured while increasing the BSA concentration from 0.2 to 1.0 mg/mL for 120 min to ensure equilibrium. The results are plotted in Figure 4A. The Q_{MIPs} increased remarkably as the initial concentration increased to 0.6 mg/mL. The trends of Sample-9-NIPs and Sample-9-MIPs were similar, but Q_{NIPs} reached equilibrium (13.0 mg/g) at only C_0 = 0.3 mg/mL. The poor performance of Sample-9-NIPs was attributed to the lack of imprinted sites on its surface, meaning that most of the protein molecules could not adsorb. The adsorption equilibrium data were also fitted by two thermodynamic adsorption models: the Langmuir isotherm and Freundlich isotherm models (see Supporting Information Table S2). Judging from the correlation coefficients, the adsorption equilibrium results of Sample-9-MIPs were better fitted by the Langmuir isotherm model than the Freundlich isotherm model (Supporting Information Table S3). This suggests that the binding sites on Sample-9-MIPs were homogeneously deposited as a monolayer.

To further study the effect of SBMA on the MIPs kinetics, the adsorption kinetics of BSA to Sample-3-MIPs and Sample-9-MIPs were determined and are shown in Figure 4B. The Q of Sample-3-MIPs reached equilibrium within 60 min,

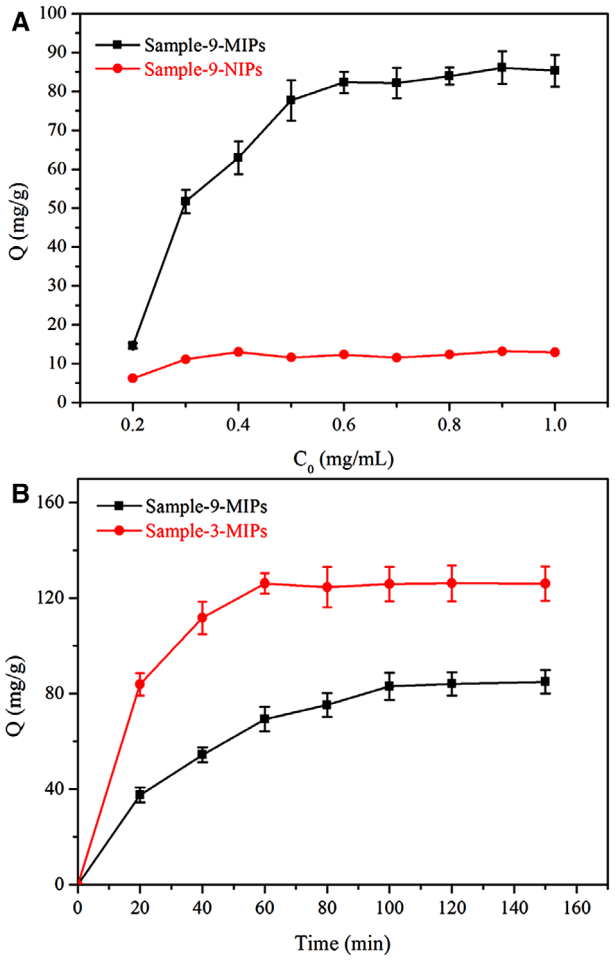

FIGURE 4 Adsorption isotherms (A) and adsorption kinetics (B) of Sample-9-MIPs and Sample-9-NIPs during BSA adsorption

but that of Sample-9-MIPs saturated after 100 min. Although the adsorption kinetics of Sample-9-MIPs and Sample-3-MIPs followed similar trends, the former achieved a higher Q than the latter. This difference is attributable to the SBMA reagent in Sample-9-MIPs, which was absent in Sample-3-MIPs. Thus, it was deduced that the SBMA chain segment

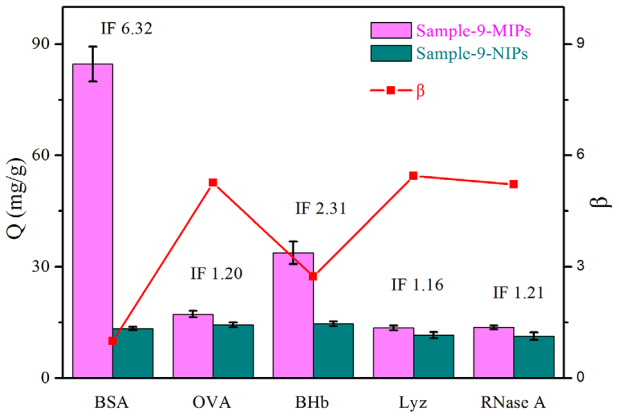

FIGURE 5 *Q* and β values of Sample-9 for BSA, OVA, BHb, Lyz, and RNase A

of Sample-9-MIPs exerted an anti-protein adsorption effect, which slowed the migration rate of the protein molecules to the imprinted sites. Therefore, to improve the *IF*, we must compromise the saturation time of the protein adsorption to the MIPs.

Figure 5 displays the *Q* and β of Sample-9-MIPs in various protein solutions. The four protein molecules in this analysis—BHb, OVA, Lyz, and RNase A—were selected for their contrastingly different isoelectric points (pIs) and molecular weights. OVA has a similar pI to BSA, but a smaller molecular weight. The Q_{MIPs} and β for OVA were 17.27 mg/g and 5.3, respectively (note that the Q_{MIPs} was lower than for BSA). According to these data, Sample-9-MIPs achieved almost no selective adsorption capacity for OVA, implying that shape memory is a dominant effect of imprinting. To further illustrate the adsorption selectivity of the MIPs, their adsorption performances to BHb were examined. BHb as a homologous protein to BSA with similar molecular weight, yet its Q_{MIPs} (33.83) and Q_{NIPs} (14.63) were lower than those of BSA, and its β was only 2.74. This situation resulted from the different pIs and distributions of surface functional groups on BSA and BHb. To further demonstrate that both shape memory and multiple non-covalent interactions between the imprinted polymer and protein molecules are essential for the imprinting effect, the adsorption performances of Sample-9-MIPs to Lyz and RNase A were examined. These protein molecules are much smaller than BSA and their pIs also differ from that of BSA. The Q_{MIPs} and Q_{NIPs} were 13.53 and 11.62, respectively for Lyz, and 13.70 and 11.32, respectively for RNAse A (lower than those of BSA), and the respective β factors were 5.45 and 5.22. To verify the specific adsorption capacity of the MIPs for BSA in a protein mixture, the adsorption performance of MIPs was studied in a mixed solution of Lyz and BSA (concentration ratio = 1:1). Finally, the initial solution and the eluent were analyzed by sodium dodecyl sulfate–polyacrylamide gel electrophoresis. Only the band of BSA appeared in Lane 4 of the eluate, indicating that the MIPs specifically recognized the target protein BSA in the mixed protein solution (Supporting Information S7).

4 | CONCLUDING REMARKS

We introduced a BSA-specific adsorption magnetic composite with excellent temperature sensitivity. MCS, *N*-isopropylacrylamide and sulfobetaine methacrylate were introduced as the functional monomers, and the Fe_3O_4 microspheres accelerated the response time to an externally applied magnetic field. The temperature sensitivity of the imprinted polymer abated the mass transfer resistance and improved the elution efficiency. When optimized, the MIPs were highly selective for BSA, with an absorption amount of 86.87 mg/g BSA and an imprinting factor of 6.49. More importantly, the specific adsorption ability was not degraded in competitive studies of mixed BSA and other protein molecules. With their excellent imprinting properties, high thermo-response sensitivity, and inexpensive recovery by magnetic separation, the prepared MIPS demonstrate huge potential in the future preparation of protein molecules.

ACKNOWLEDGMENTS

The authors are grateful for the financial support provided by the State Key Program of National Natural Science Foundation of China (Grant No. 51433008), the National Natural Science Foundation of China (Grant No. 21704084) and the Fundamental Research Funds for the Central Universities (Grant No. 3102017jc01001).

CONFLICT OF INTEREST

The authors have declared no conflict of interest.

ORCID

Qiuyu Zhang https://orcid.org/0000-0002-4823-5031

REFERENCES

1. Wackerlig, J., Schirhagl, R., Applications of molecularly imprinted polymer nanoparticles and their advances toward industrial use: A review. *Anal. Chem.* 2016, *88*, 250–261.
2. Wulff, G., Molecular imprinting in crosslinked materials with the aid of molecular templates-a way towards artificial antibodies. *Angew. Chem. Int. Ed.* 1995, *34*, 1812–1832.
3. Yang, H., Li, L., Ding, Y., Ye, D., Wang, Y., Cui, S., Liao, L., Molecularly imprinted electrochemical sensor based on bioinspired Au microflowers for ultra-trace cholesterol assay. *Biosens. Bioelectron.* 2017, *92*, 748–754.
4. Brandis, A., Partouche, E., Yechezkel, T., Salitra, Y., Shkoulev, V., Scherz, A., Grynszpan, F., A two-step strategy to visually identify

molecularly imprinted polymers for tagged proteins. *J. Sep. Sci.* 2017, *40*, 3358–3367.
5. Zhou, J., Wang, Y., Ma, Y., Zhang, B., Zhang, Q., Surface molecularly imprinted thermo-sensitive polymers based on light-weight hollow magnetic microspheres for specific recognition of BSA. *Appl. Surf. Sci.* 2019, *486*, 265–273.
6. Qian, L., Yang, M., Chen, H., Xu, Y., Zhang, S., Zhou, Q., He, B., Bai, Y., Song, W., Preparation of a poly(ionic liquid)-functionalized cellulose aerogel and its application in protein enrichment and separation. *Carbohydr. Polym.* 2019, *218*, 154–162.
7. Zhang, Z., Li, L., Efficient synthesis of molecularly imprinted polymers with bio-recognition sites for the selective separation of bovine hemoglobin. *J. Sep. Sci.* 2018, *41*, 2479–2487.
8. Yaqub, S., Latif, U., Dickert, F. L., Plastic antibodies as chemical sensor material for atrazine detection. *Sensor. Actuat. B-Chem.* 2011, *160*, 227–233.
9. Tamahkar, E., Bereli, N., Say, R., Denizli, A., Molecularly imprinted supermacroporous cryogels for cytochrome c recognition. *J. Sep. Sci.* 2011, *34*, 3433–3440.
10. Chen, L., Xu, S., Li, J., Recent advances in molecular imprinting technology: Current status, challenges, and highlighted applications. *Chem. Soc. Rev.* 2011, *40*, 2922–2942.
11. Tang, L., Zhao, C. Y., Wang, X. H., Li, R. S., Yang, J. R., Huang, Y. P., Liu, Z. S., Macromolecular crowding of molecular imprinting: A facile pathway to produce drug delivery devices for zero-order sustained release. *Int. J. Pharm.* 2015, *496*, 822–833.
12. Zaidi, S. A., Molecular imprinted polymers as drug delivery vehicles. *Drug Deliv.* 2016, *23*, 2262–2271.
13. Li, X., Zhang, B., Li, W., Lei, X., Fan, X., Tian, L., Zhang, H., Zhang, Q., Preparation and characterization of bovine serum albumin surface-imprinted thermosensitive magnetic polymer microsphere and its application for protein recognition. *Biosens. Bioelectron.* 2014, *51*, 261–267.
14. Qian, L., Sun, J., Hou, C., Yang, J., Li, Y., Lei, D., Yang, M., Zhang, S., Immobilization of BSA on ionic liquid functionalized magnetic Fe_3O_4 nanoparticles for use in surface imprinting strategy. *Talanta* 2017, *168*, 174–182.
15. Ge, Y., Turner, A. P., Too large to fit? Recent developments in macromolecular imprinting. *Trends Biotechnol.* 2008, *26*, 218–224.
16. Wang, Y., Zhou, J., Wu, C., Tian, L., Zhang, B., Zhang, Q., Fabrication of micron-sized BSA-imprinted polymers with outstanding adsorption capacity based on poly(glycidyl methacrylate)/polystyrene (PGMA/PS) anisotropic microspheres. *J. Mater. Chem. B* 2018, *6*, 5860–5866.
17. Bie, Z., Chen, Y., Ye, J., Wang, S., Liu, Z., Boronate-Affinity Glycan-Oriented surface imprinting: A new strategy to mimic lectins for the recognition of an intact glycoprotein and its characteristic fragments. *Angew. Chem. Int. Ed. Engl.* 2015, *54*, 10211–10215.
18. Xu, S., Lu, H., Ratiometric fluorescence and mesoporous structure dual signal amplification for sensitive and selective detection of TNT based on MIP@QD fluorescence sensors. *Chem. Commun.* 2015, *51*, 3200–3203.
19. Kitayama, Y., Isomura, M., Gas-stimuli-responsive molecularly imprinted polymer particles with switchable affinity for target protein. *Chem. Commun.* 2018, *54*, 2538–2541.
20. Bertolla, M., Cenci, L., Anesi, A., Ambrosi, E., Tagliaro, F., Vanzetti, L., Guella, G., Bossi, A. M., Solvent-responsive molecularly imprinted nanogels for targeted protein analysis in MALDI-TOF mass spectrometry. *ACS Appl. Mater. Inter.* 2017, *9*, 6908–6915.
21. Xie, J., Zhong, G., Cai, C., Chen, C., Chen, X., Rapid and efficient separation of glycoprotein using pH double-responsive imprinted magnetic microsphere. *Talanta* 2017, *169*, 98–103.
22. Zhang, M., Zhang, X., He, X., Chen, L., Zhang, Y., A self-assembled polydopamine film on the surface of magnetic nanoparticles for specific capture of protein. *Nanoscale* 2012, *4*, 3141–3147.
23. Guo, H., Yuan, D., Fu, G., Enhanced surface imprinting of lysozyme over a new kind of magnetic chitosan submicrospheres. *J. Colloid. Interface. Sci.* 2015, *440*, 53–59.
24. Zhu, X., Li, H., Liu, H., Peng, W., Zhong, S., Wang, Y., Halloysite-based dopamine-imprinted polymer for selective protein capture. *J. Sep. Sci.* 2016, *39*, 2431–2437.
25. Li, X., Zhou, J., Tian, L., Wang, Y., Zhang, B., Zhang, H., Zhang, Q., Preparation of anti-nonspecific adsorption polydopamine-based surface protein-imprinted magnetic microspheres with the assistance of 2-methacryloyloxyethyl phosphorylcholine and its application for protein recognition. *Sensor. Actuat. B-Chem.* 2017, *241*, 413–421.
26. Luan, J., Liu, K. K., Tadepalli, S., Jiang, Q., Morrissey, J. J., Kharasch, E. D., Singamaneni, S., PEGylated artificial antibodies: Plasmonic biosensors with improved selectivity. *ACS Appl. Mater. Inter.* 2016, *8*, 23509–23516.
27. Ma, Y., Ma, M., Yin, X., Shao, Q., Lu, N., Feng, Y., Lu, Y., Wujcik, E. K., Mai, X., Wang, C., Guo, Z., Tuning polyaniline nanostructures via end group substitutions and their morphology dependent electrochemical performances. *Polymer* 2018, *156*, 128–135.
28. Li, D., Liu, L., Tian, K., Liu, J., Fan, X., Synthesis, biodegradability and cytotoxicity of water-soluble isobutylchitosan. *Carbohydr. Polym.* 2007, *67*, 40–45.
29. Spector, T., Refinement of the Coomassie blue method of protein quantitation: A simple and linear spectrophotometric assay for $\leq$ 0.5 to 50 μg of protein. *Anal. biochem.* 1978, *86*, 142–146.
30. Wang, S., Xie, F., Wu, X., Ma, Y., Du, H., Wu, G., Cathodic plasma electrolytic deposition of ZrO_2/YSZ doped Al_2O_3 ceramic coating on TiAl alloy. *Ceram. Int.* 2019, *45*, 18899–18907.
31. Ma, Y., Hou, C., Zhang, H., Qiao, M., Chen, Y., Zhang, H., Zhang, Q., Guo, Z., Morphology-dependent electrochemical supercapacitors in multi-dimensional polyaniline nanostructures. *J. Mater. Chem. A* 2017, *5*, 14041–14052.

SUPPORTING INFORMATION

Additional supporting information may be found online in the Supporting Information section at the end of the article.

How to cite this article: Wang Y, Ma Y, Zhou J, Su K, Zhang B, Zhang Q. Thermo-sensitive surface molecularly imprinted magnetic microspheres based on bio-macromolecules and their specific recognition of bovine serum albumin. *J Sep Sci* 2020;43:996–1002. https://doi.org/10.1002/jssc.201901024